DALTON
FULL PAPER

Crystal structures, magnetic and spectroscopic properties of manganese(II), cobalt(II), nickel(II) and zinc(II) dichloro complexes bearing two 2-pyridyl-substituted imino nitroxides †

Youhei Yamamoto, Takayoshi Suzuki and Sumio Kaizaki *

Department of Chemistry, Graduate School of Science, Osaka University, Toyonaka 560-0043, Japan

Received 22nd December 2000, Accepted 23rd March 2001
First published as an Advance Article on the web 23rd April 2001

Four new complexes of formula $[MCl_2(IM2py)_2]$, where M = Mn(II), Co(II), Ni(II) or Zn(II); IM2py = 4,4,5,5-tetramethyl-2-(2-pyridyl)-imidazolin-1-oxyl, have been prepared, and examined from viewpoints of the crystal structures, magnetic and spectroscopic properties. All the complexes crystallize in an isomorphous space group $C2/c$ with $Z = 4$, and exist as discrete mononuclear molecules with *OC*-6-22 [*cis*(Cl)-*trans*(py)] geometrical structure in the crystal. In the zinc(II) complex a moderate intramolecular IM2py–IM2py antiferromagnetic interaction ($2J' = -19.1(1)$ cm^{-1}) is estimated by the magnetic susceptibility measurement. The magnetic interactions between Mn(II) and IM2py are found to be antiferromagnetic, $J = -23.8(2)$ cm^{-1}. Ferromagnetic interactions of the complexes of Ni(II) and Co(II) are inferred from the magnetic susceptibility. These magnetic properties are substantiated by the variable temperature UV-vis-NIR spectra of which the intensities increase for Mn(II) or decrease for Ni(II) and Co(II) with decreasing temperature for the spin-forbidden d–d transition and/or the metal(II) dσ to IM2py SOMO π* CT transition.

Introduction

There have been a large number of investigations on transition metal complexes of the nitronyl nitroxide NITR (2-R-4,4,5,5-tetramethylimidazolin-1-oxyl 3-oxide), aiming at the so-called metal–radical approach for molecular magnets.[1–14] On the other hand, only a few papers have dealt with spectroscopic aspects in connection with the magnetic properties.[15–17] We have demonstrated the spin-forbidden transition intensity enhancements of complexes of Cr(III) and Ni(II) with NIT2py (Scheme 1)[15] and

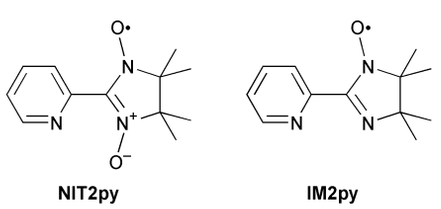

NIT2py IM2py

Scheme 1 The nitronyl and imino nitroxides.

the relations of the antiferromagnetic exchange constants with the spin-forbidden d–d transition intensities[15] or NMR contact shifts[16] in the NIT2py complexes of Ni(II) with various kinds of β-diketonates. The UV-vis and luminescence spectral changes on co-ordination of an NIT radical were also discussed for the gadolinium(III) complex.[17] As another type of spin coupled system, di-, tri-, tetra-[18] and one-dimensional ferrimagnet polynuclear[19] complexes with paramagnetic copper(II) and manganese(II) ions have been studied in connection with magneto-optical devices where the spin-forbidden transition intensity enhancements on cooling were examined in a quantitative manner. However, there has been no study on the magneto-optical properties of metal complexes which give spin-forbidden transition intensity enhancement on warming, or the ferromagnetic interaction. For this purpose, the imino nitroxide IM2py [4,4,5,5-tetramethyl-2-(2-pyridyl)imidazolin-1-oxyl: Scheme 1] complexes seems to be appropriate, because it is generally found in such complexes having magnetic dσ orbitals such as [(Cu or Ni)(hfac)$_2$(IM2py)] (hfac = 1,1,1,6,6,6-hexafluoropentane-2,4-dionate) that there is a ferromagnetic interaction between Cu(II) or Ni(II) and IM2py,[20,21] in contrast to a strong antiferromagnetic interaction in the corresponding NIT2py complexes.[2,5] The ferromagnetism of the IM2py complexes is rationalized by considering the exchange coupling of the metal dσ and radical unpaired electrons in the orthogonal magnetic orbitals, owing to a planar five-membered chelate ring formed by IM2py.[20] In view of possible co-ordination of the imino nitroxides *via* an imino-N atom to a metal centre which could force the nearby ligating site sterically crowded by the α-*gem*-dimethyl group into close contact with another ligand,[21] the molecular structures of the IMR complexes are often remarkably different from those of the NITR complexes.[20–27] While Luneau *et al.*[2] and other research groups[3,4] have reported the syntheses, crystal structures and magnetic properties of transition metal(II) dichloro complexes bearing NIT2py, there has been no report on the corresponding IM2py complexes so far. These points prompted us to compare the structures and magnetic or spectroscopic properties between IM2py complexes and the reported NIT2py complexes.

We will deal with the dichloro complexes of Mn(II), Co(II), Ni(II) and Zn(II) containing IM2py, $[MCl_2(IM2py)_2]$ (M = Mn **1**, Co **2**, Ni **3** or Zn **4**).

Experimental

Preparation

The nitroxide, IM2py, was prepared by the literature method.[28]

Diethyl ether vapour was diffused into a methanol solution (3 cm^3) containing $MnCl_2 \cdot 4H_2O$ (0.50 mmol) and IM2py

† Electronic supplementary information (ESI) available: perspective drawings of complexes **2**–**4**, temperature-dependent vis-NIR spectra of **1** and **2**, equations used in magnetic susceptibility data analysis. See http://www.rsc.org/suppdata/dt/b0/b010243l/

 DOI: 10.1039/b010243l

Table 1 Crystal data for complexes $[MCl_2(IM2py)_2]$ (M = Mn **1**, Co **2**, Ni **3** or Zn **4**)

	1	**2**	**3**	**4**
Formula	$C_{24}H_{32}Cl_2MnN_6O_2$	$C_{24}H_{32}Cl_2CoN_6O_2$	$C_{24}H_{32}Cl_2N_6NiO_2$	$C_{24}H_{32}Cl_2N_6O_2Zn$
M	562.40	566.40	566.16	572.84
T/°C	23	20	20	23
Crystal system	Monoclinic	Monoclinic	Monoclinic	Monoclinic
Space group	$C2/c$ (no. 15)	$C2/c$ (no. 15)	$C2/c$ (no. 15)	$C2/c$ (no. 15)
Z	4	4	4	4
a/Å	18.454(2)	18.5308(8)	18.604(1)	18.550(3)
b/Å	9.156(2)	8.9969(5)	8.9489(6)	9.122(2)
c/Å	15.835(2)	15.931(1)	15.633(3)	15.806(2)
β/°	100.856(8)	101.837(4)	102.633(3)	102.46(1)
U/Å^3	2627.6(7)	2599.5(2)	2587.7(3)	2611.4(6)
μ(Mo-Kα)/mm^{-1}	0.739	0.899	0.993	1.179
Refln./param.	3846/163	2807/163	2815/163	3817/163
$R1\{F^2; F^2 > 2\sigma(F^2)\}$	0.038	0.036	0.035	0.033
$wR(F^2$; all data)	0.110	0.090	0.088	0.093

(1.00 mmol) in a desiccator at room temperature, affording brown plate crystals of $[MnCl_2(IM2py)_2]$ **1**. The crystals were collected by filtration and dried in air (60%) (Found: C, 51.18; H, 5.77; N, 14.87. $C_{24}H_{32}Cl_2MnN_6O_2$ requires C, 51.26; H, 5.74; N, 14.97%). mp (decomp.) > 300 °C. Brown plate crystals of $[CoCl_2(IM2py)_2]$ **2**, 50% (Found: C, 50.14; H, 5.64; N, 14.54. $C_{24}H_{32}Cl_2CoN_6O_2$ requires C, 50.89; H, 5.69; N, 14.84%), mp 220 °C, and red-brown plate crystals of $[NiCl_2(IM2py)_2]$ **3**, 70% (Found: C, 50.60; H, 5.82; N, 14.43. $C_{24}H_{32}Cl_2N_6NiO_2$ requires C, 50.92; H, 5.70; N, 14.84%), mp (decomp.) > 280 °C, were obtained by a similar method with use of $CoCl_2{\cdot}6H_2O$ and $NiCl_2{\cdot}6H_2O$, respectively. Orange-red plate crystals of $[ZnCl_2(IM2py)_2]$ **4** were obtained from a reaction of $ZnCl_2$ and an excess amount of IM2py in acetonitrile (80%) (Found: C, 50.27; H, 5.62; N, 14.76. $C_{24}H_{32}Cl_2N_6O_2Zn$ requires C, 50.32; H, 5.63; N, 14.67%), mp 155 °C.

Crystallography

The X-ray intensities of complexes **1** and **4** were measured on a Rigaku automated four-circle diffractometer AFC-5R or AFC-7R [graphite monochromated Mo-Kα radiation (λ = 0.71073 Å), ω–2θ scan, $2\theta_{max}$ = 60°], those of **2** and **3** on a Rigaku imaging plate area detector R-AXIS Rapid [graphite monochromated Mo-Kα radiation (λ = 0.71073 Å), $2\theta_{max}$ = 55°]. The structures were solved by the direct method using the SHELXS 86 program[29] and refined on F^2 by full-matrix least squares using SHELXL 97.[30] Crystal data are summarized in Table 1.

CCDC reference numbers 161343–161346.

See http://www.rsc.org/suppdata/dt/b0/b010243l/ for crystallographic data in CIF or other electronic format.

Measurements

The magnetic susceptibility data were collected with a SQUID-based sample magnetometer on a QUANTUM design model MPMS instrument. Data were corrected for magnetization of the sample holder and for the diamagnetic contributions, which were estimated from Pascal's constants. UV-vis spectra were measured on a Perkin-Elmer Lambda 19 spectrophotometer. An Oxford liquid nitrogen cryostat model DN1704 and a temperature controller ITC 502 were used for the temperature-dependent measurements.

Results and discussion

Crystal structures of complexes

Single-crystal X-ray analysis revealed that the complexes **1**–**4** crystallize in an isomorphous space group $C2/c$ with Z = 4. Their molecular and crystal structures are similar to one another, where the central metal atom (M) lies on a crystallographic

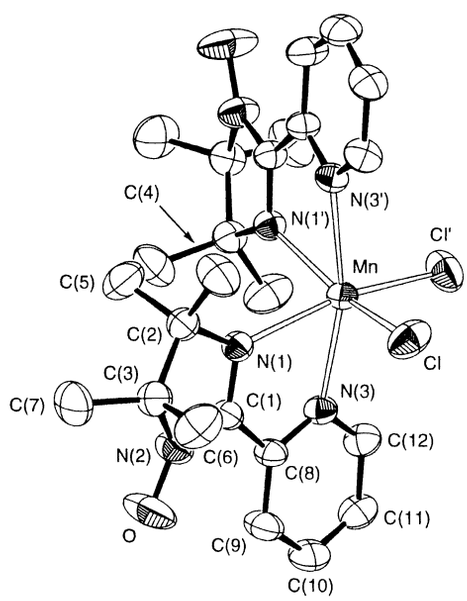

Fig. 1 Perspective drawing of (*OC*-6-22)-$[MnCl_2(IM2py)_2]$ **1**. Hydrogen atoms are omitted for clarity, and the thermal ellipsoids are drawn at 50% probability level.

C_2 axis. A perspective view of the manganese(II) complex **1** is depicted in Fig. 1 (those of the other complexes are deposited as ESI Fig. S1). The co-ordination geometry around the M(II) can be described as *OC*-6-22 [*cis*(Cl)-*trans*(py) isomer], which is in contrast to the *OC*-6-12 [*trans*(Cl)-*trans*(py)] structure found in the analogous complexes $[MCl_2(NIT2py)_2]$ {M = Mn(II), Ni(II),[2] Cu(II)[4] or Co(II)[31]}. The IM2py co-ordinates to an M(II) *via* the pyridyl- and imino-N atoms to form a planar five-membered chelate ring as found in $[(Ni\ or\ Cu)(hfac)_2(IM2py)]$.[20,21] The chelate ring is almost coplanar not only to the pyridyl ring but also to the imino nitroxide moiety (Table 2). This coplanarity seems to be a key factor for determining the different geometrical structures between the IM2py and the NIT2py ones. That is, the *trans*(Cl) isomers of $[MCl_2(IM2py)_2]$ are unfavourable due to the steric hindrance arising from the α-*gem*-dimethyl group upon imino-N co-ordination. The *trans*(py) geometrical structure around Ni(II) of the present dichloro complex **3** is also found for the recently reported nickel(II) moiety in $[\{Ni(IM2py)_2\}_3\{Fe(CN)_6\}_2]$.[25]

Table 2 compares selected structural parameters of complexes **1**–**4**. Those of the IM2py moiety are very similar to one another and to those of $[(Ni\ or\ Cu)(hfac)_2(IM2py)]$;[20,21] the N–O bond lengths are in the range of 1.265(2)–1.271(2) Å. The bite angle of the IM2py chelate varies from 70.97(6) of **1** to 77.56(5)° of **3**, but this variation seems to result from the difference in the M–N(1) and M–N(3) bond lengths. The deviation of

Table 2 Selected structural parameters (*l*/Å, *φ*/°) for complexes $[MCl_2(IM2py)_2]$ (M = Mn **1**, Co **2**, Ni **3** and Zn **4**)

	1	**2**	**3**	**4**
M–Cl	2.4509(8)	2.4087(6)	2.4132(5)	2.3671(7)
M–N(1)	2.359(2)	2.213(2)	2.157(1)	2.352(2)
M–N(3)	2.304(2)	2.172(2)	2.111(1)	2.177(2)
N(2)–O	1.265(2)	1.269(2)	1.271(2)	1.266(2)
N(1)–M–N(3)	70.97(6)	75.32(6)	77.56(5)	73.20(6)
Cl–M–Cl′	101.03(4)	99.92(4)	97.24(3)	102.82(4)
N(1)–M–N(1′)	90.91(9)	91.40(9)	93.24(8)	86.98(8)
N(3)–M–N(3′)	164.89(9)	172.40(9)	174.44(8)	162.99(9)
M–N(1)–C(1)–N(2)	169.2(2)	169.0(2)	170.6(1)	168.2(1)
Plane MN_2[a] *vs.* plane im[b]	10.68(5)	10.40(7)	8.84(8)	12.04(6)
Plane MN_2[a] *vs.* plane py[c]	12.64(6)	7.96(6)	6.68(5)	10.37(5)
Plane im[b] *vs.* plane py[c]	3.0(2)	3.9(2)	4.1(2)	2.9(2)
Shortest intermolecular O · · · O distance	5.567(5)	5.558(4)	5.559(4)	5.558(5)

[a] Defined by M, N(1) and N(3). [b] Defined by O, N(1), C(1) and N(2). [c] Defined by N(3), C(8), C(9), C(10), C(11) and C(12).

M–Cl, M–N(1) and M–N(3) bond lengths among complexes **1**–**4** cannot necessarily be accounted for in a simple way by the ionic radii of the metal(II) ions; Mn(II), 0.970; Co(II), 0.885; Ni(II), 0.83; Zn(II), 0.88 Å.[32] In particular, the Zn–N(1) bond length is remarkably longer than the Co–N(1), suggesting a weaker Zn(II)–imino-N bond than the other M(II)–imino-N. The N(3)–M–N(3′) bonds are not linear, but 162.99(9)–174.44(8)°, probably owing to the smaller bite angle of IM2py than the right angle. On the other hand, the Cl–M–Cl′ bond angle [97.24(3)–102.82(4)°] is relatively larger than 90°.

In contrast to a dimer unit of [(Ni or Cu)(hfac)$_2$(IM2py)] with a short intermolecular N–O · · · O–N contact in the crystal structures,[20,21] the present complexes $[MCl_2(IM2py)_2]$ with the shortest intermolecular O · · · O distance of more than 5.5 Å are considered to be discrete mononuclear molecules in the crystals.

Any attempts to prepare the corresponding complexes of Fe(II) and Cu(II) were unsuccessful. In the case of Cu(II), the difficulty to form the desired complex may arise from the steric influence or the *cis* co-ordination of two IM2py chelates associated with the Jahn–Teller distortion expected for copper(II) complexes. The reaction of $FeCl_2 \cdot 4H_2O$ and IM2py led to decomposition of IM2py, giving a complicated mixture of uncharacterizable compounds.

Magnetic properties

$[ZnCl_2(IM2py)_2]$. The temperature dependence of the molar magnetic susceptibility (χ_m) and the $\chi_m T$ product for complex **4** are shown in Fig. 2. The $\chi_m T$ product (0.758 cm^3 K mol^{-1} at 300 K) decreased on lowering the temperature pointing to a singlet ground state and a moderate antiferromagnetic interaction. Below T_{max} (17 K) where the χ_m value showed a maximum, χ_m decreased to reach a minimum value 0.198×10^{-2} cm^3 mol^{-1} at 3.25 K and then increased on further cooling (Fig. 2, inset). This non-zero value of χ_m at the lowest temperature is due to the presence of paramagnetic impurities in the sample. It is possible that the paramagnetic impurity is a tetrahedral four-co-ordinate mono(IM2py) species, $[ZnCl_2(IM2py)]$, which is not neglected in view of the formation of the corresponding four-co-ordinate complexes with NIT2py[31] and 6-methylpyridyl derivatives (NITmepy and IMmepy).[33] Taking this contamination into account, the temperature variation of χ_m was analysed over the whole temperature range measured (the eqn. S1 for the analysis is given as ESI). Assuming that the g_R values of both bis- and mono-IM2py complexes are equal to 2, the least-squares fitting gave the best fit parameters of $2J' = -19.1(1)$ cm^{-1} ($H = -2J'\boldsymbol{S}_{R1} \cdot \boldsymbol{S}_{R2}$) and ρ (impurity factor) = 0.0134(9) [R $\{= \Sigma(\chi_{calc} - \chi_{obs})^2/\Sigma\chi_{obs}^2\} = 1.8 \times 10^{-3}$]. Since the zinc(II) complex exists as a discrete molecule in the crystal, the antiferromagnetism must originate from the intramolecular interaction between two IM2py radicals.

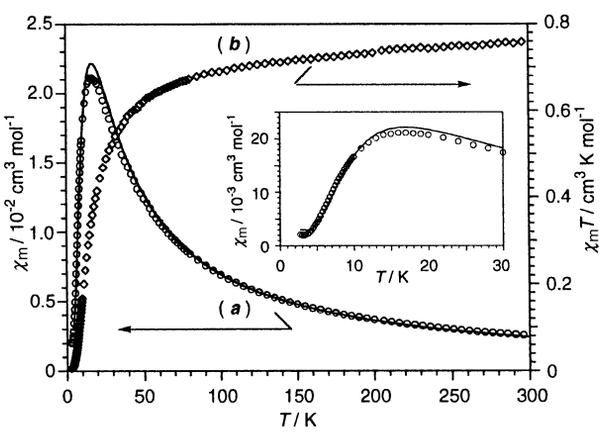

Fig. 2 Temperature dependence of the magnetic susceptibility for complex **4** in the forms (*a*) χ_m *vs.* T and (*b*) $\chi_m T$ *vs.* T. The solid line represents the best-fit calculated data. The inset shows an expansion of the low-temperature region.

Of the through-space and through-bond paths for transmission of the antiferromagnetic interaction, the former direct path is plausible for the present case rather than the latter *via* the diamagnetic zinc(II) centre as follows. No observable absorption band corresponding to the zinc(II) dπ to IM2py SOMO π*(N–O) CT transition in the region up to 42000 cm^{-1} (*vide infra*) suggests that the location of zinc(II) dπ orbitals is too low in energy to mediate the magnetic interaction between two imino nitroxide radicals by the through-bond path. This is in line with the very recent case of $[Zn(2,6\text{-}NIT_2py)_2][ClO_4]_2 \cdot 2.5CH_3CN$ {2,6-NIT_2py = 2,6-bis(4,4,5,5-tetramethylimidazolin-1-oxyl-2-yl 3-oxide)pyridine}.[13] It is claimed that the antiferromagnetic interactions between proximate nitronyl nitroxide radicals are propagated through space rather than the through-bond path by which magnetic interactions are promoted with difficulty owing to the high energy CT states. Therefore, the intramolecular antiferromagnetism between neighbouring IM2py ligands would originate from the through-space interaction. This is in contrast to the analogous case of the palladium(II) complex *trans*-$[PdCl_2(IMmepy)_2]$, with $2J' = -168.0$ cm^{-1},[26] where an intramolecular coupling between two imino nitroxides *via* a filled dπ orbital of diamagnetic Pd(II) has been postulated by Oshio *et al.*

$[MnCl_2(IM2py)_2]$. The $\chi_m T$ product (4.21 cm^3 K mol^{-1}) of the manganese(II) complex **1** at 300 K is smaller than the

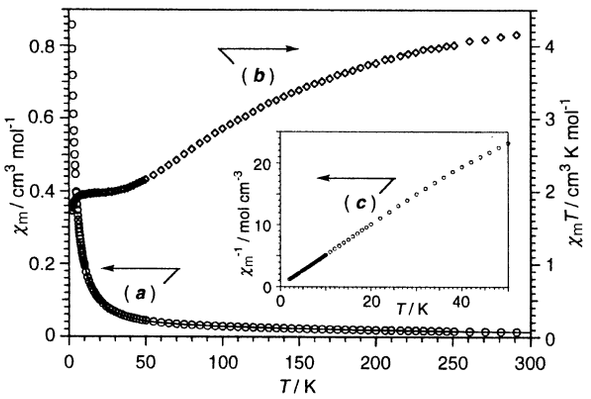

Fig. 3 Temperature dependence of the magnetic susceptibility for complex **1** in the forms (*a*) χ_m *vs.* T, (*b*) $\chi_m T$ *vs.* T and (*c*) χ_m^{-1} *vs.* T. The solid line represents the best-fit calculated data.

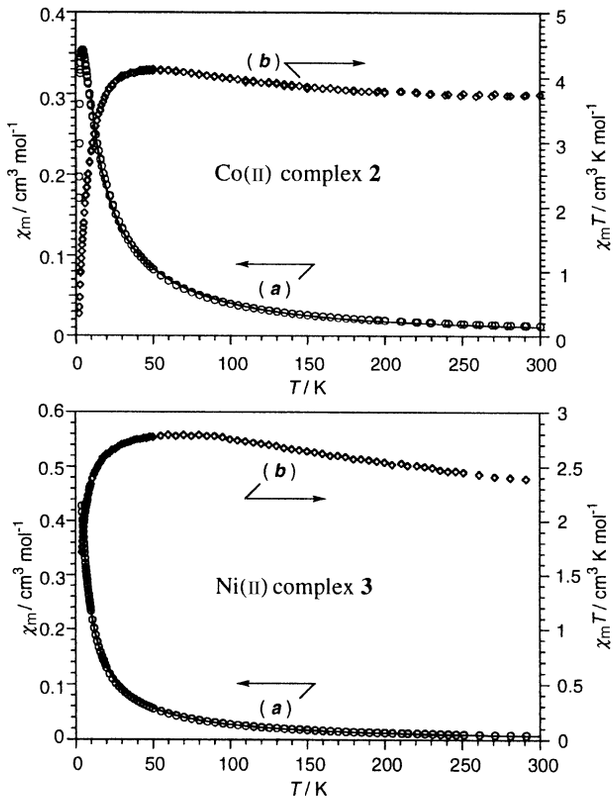

Fig. 4 Temperature dependence of the magnetic susceptibilities for complexes **2** and **3** in the forms (*a*) χ_m *vs.* T and (*b*) $\chi_m T$ *vs.* T. The solid line represents the best-fit calculated data.

expected value (5.125 cm^3 K mol^{-1} for $g_{Mn} = g_R = 2$) for independent spins system ($S_{Mn} = \frac{5}{2}$ and $S_{R1} = S_{R2} = \frac{1}{2}$). The $\chi_m T$ product decreased with decreasing temperature, and gave a plateau around 40 K (Fig. 3). The $\chi_m T$ value of the plateau at 10 K was 1.95 cm^3 K mol^{-1}, corresponding to $S = \frac{3}{2}$. These facts indicate antiferromagnetic interactions between Mn(II) and two IM2py radicals with the ground quartet state characterized as $|S,\ S_R\rangle = |\frac{3}{2},\ 1\rangle$ $\{S = S_{Mn} + S_R = S_{Mn} + (S_{R1} + S_{R2})\}$. In order to neglect any intermolecular interaction, the temperature variation of χ_m at $T \geq 10$ K was analysed on the basis of the isotropic spin Hamiltonian $H = -2J\ S_{Mn}(S_{R1} + S_{R2}) - 2J'\ S_{R1}\cdot S_{R2}$ (see eqn. S2 of ESI). Assuming $g_R = 2$ and using $2J' = -19.1$ cm^{-1} estimated for the intramolecular interaction in the zinc(II) complex **4**, the parameter values were estimated to be $g_{Mn} = 2.033(1)$ and $J = -23.8(2)$ cm^{-1} by least-squares fitting ($R = 5.4 \times 10^{-5}$). The antiferromagnetic interaction between Mn(II) and IM2py gives the lowest excited state $|\frac{5}{2}, 1\rangle$. The next lowest excited state of $|\frac{5}{2}, 0\rangle$ is higher in energy by $2J + 2J'$ than $|\frac{5}{2}, 1\rangle$, so that J' remains nearly independent in the fitting process. In fact, for $J' = 0$ cm^{-1}, the resultant J value [$-23.1(2)$ cm^{-1}] remained almost unchanged. The estimated antiferromagnetic interaction ($J = -23.8$ cm^{-1}) between Mn(II) and IM2py of complex **1** is smaller compared to that of the analogous NIT2py complex, $[MnCl_2(NIT2py)_2]$ ($J = -79$ cm^{-1}).[2] This results mainly from the difference in the co-ordination structures between NIT2py and IM2py chelates. Owing to the coplanarity of the imino nitroxide moiety to the manganese(II) co-ordination plane, the SOMO of IM2py gives an effective π-type overlap with one of the dπ orbitals, and is orthogonal to the other dπ and two dσ orbitals of Mn(II). In contrast, NIT2py co-ordinates to form a puckered six-membered chelate ring,[2] which induces the SOMO of NIT2py to have effective σ- and π-type couplings with all the dσ and dπ orbitals of Mn(II). Therefore, a much less antiferromagnetic contribution from the five d electrons of Mn(II) is realized for the IM2py complex than the NIT2py one as expected.

A plateau in the $\chi_m T$ *versus* T plot indicates that the thermal population exists within the ground quartet state below 40 K as in Fig. 3. Therefore, a sharp decrease of $\chi_m T$ below 4 K is due either to zero-field splitting or to the intermolecular antiferromagnetic coupling of the ground quartet state. The zero-field splitting could be neglected, since the dominant local anisotropy tensor of the ground quartet state, D_{Mn}, is practically too small to give zero-field splitting.[1,34] Hence, a sharp decrease of $\chi_m T$ toward lower temperature is attributed to the intermolecular magnetic interaction. From a plot of reciprocal susceptibility (χ_m^{-1}) against T (Fig. 3, inset), a Curie–Weiss law holds at temperatures below 20 K, and the Weiss temperature is found to be $\theta = -0.28$ K. This very weak interaction results from the shortest intermolecular O···O distance of more than 5.55 Å between discrete molecules in the crystal as evidenced by the X-ray analysis.

$[NiCl_2(IM2py)_2]$. The magnetic properties of complex **3** with the intramolecular IM2py–IM2py interaction as well as the Ni(II)–IM2py one are of interest compared with the reported large ferromagnetic properties in $[Ni(hfac)_2(IM2py)]$ ($2J = +190$ cm^{-1})[21] and the Ni(II)–Fe(III) cluster $[\{Ni(IM2py)_2\}_3\{Fe(CN)_6\}_2]$ ($2J = +200$–300 cm^{-1}).[26]

The χ_m *versus* T and $\chi_m T$ *versus* T plots of complex **3** are shown in Fig. 4. The $\chi_m T$ product gradually increased to the maximum (2.79 cm^3 K mol^{-1}) at 70 K, and decreased sharply to 1.71 cm^3 K mol^{-1} at 4 K. The temperature variation of χ_m was analysed according to the isotropic spin Hamiltonian $H = -2J\ S_{Ni}(S_{R1} + S_{R2}) - 2J'S_{R1}\cdot S_{R2}$ (see eqn. S3 in ESI). Assuming $g_R = 2$ and $2J' = -19.1$ cm^{-1} for complex **1**, the least-squares fitting ($R = 1.9 \times 10^{-4}$) gave $g_{Ni} = 2.024(7)$, $2J = 134(10)$ cm^{-1} and $\theta = -3.00(3)$ K. The fairly large ferromagnetic interaction between Ni(II) and IM2py is also inferred from the dominant population of the ground quintet state even at room temperature as seen for the spectroscopic behaviour (*vide infra*). In this analysis the resultant intermolecular interaction parameter (θ) is much larger than that of the manganese(II) complex **1**. However, since **3** is isomorphous to **1**, the intermolecular coupling in complex **3** should be as weak as that in **1**. Therefore, a remarkable decrease of the $\chi_m T$ product below 20 K is due either to the zero-field splitting or to spin–orbit coupling. Attempts at further analysis including two such terms have been unsuccessful so far.

$[CoCl_2(IM2py)_2]$. The χ_m *versus* T and $\chi_m T$ *versus* T plots of complex **2** are shown in Fig. 4. The $\chi_m T$ increased gradually with decreasing temperature, similarly to that of the nickel(II) complex **3**. This suggests the existence of ferromagnetic interaction between Co(II) and IM2py in **2**.

For octahedral cobalt(II) complexes the orbital contribution must generally be included in order to interpret the low-

temperature magnetic behaviour. Since it is difficult to make an analysis with the orbital contribution, the higher temperature magnetic susceptibility data above 50 K were simulated on the basis of the simple isotropic spin Hamiltonian $\boldsymbol{H} = -2J\boldsymbol{S}_{Co}(\boldsymbol{S}_{R1} + \boldsymbol{S}_{R2}) - 2J'\boldsymbol{S}_{R1}\cdot\boldsymbol{S}_{R2}$ (see eqn. S4 in ESI). During the fitting process g_R and $2J'$ were set to be 2 and -19.1 cm^{-1}, respectively, for complex **1** and g_{Co}, J, and θ were parameterized. The least-squares fitting gave $g_{Co} = 2.431(6)$, $J = 14.9(6)$ cm^{-1} and $\theta = -7.2(3)$ K. As for the nickel(II) complex **3**, the θ value is estimated to be rather larger than the expected one from the crystal structure, the inconsistent data at low temperature being due to spin–orbit coupling and zero-field splitting.

Among three examples of cobalt(II) complexes with more than one NIT radical centre, two show antiferromagnetic interactions,[12,13] whereas the remaining one, *cis*-[Co(hfac)$_2$(NITPhMe)$_2$] [NITPhMe = 4,4,5,5-tetramethyl-2-(4-methylphenyl)imidazolin-1-oxyl 3-oxide], is ferromagnetic.[7] For the latter it was claimed that the lowest energy virtual ferromagnetic CT excited state was responsible for the ferromagnetic interaction.[7] However, in complex **2**, variable temperature visible absorption spectra indicate that the lowest energy CT state has the antiferromagnetic configuration with a spin quartet (*vide infra*). Therefore, such an approach alone could not interpret the magnetic properties in complex **2**. Examination of the magnetic orbitals in the dπ (t_{2g}) subshell of Co(II) may make it possible to account for fairly moderate ferromagnetic interaction as follows. Under the C_2 or holoherized D_{4h} symmetry of complex **2**, three dπ (t_{2g}) orbitals are split into one degenerate (e_g) and one non-degenerate (b_{2g}) orbital. If the b_{2g} orbital could be located at higher energy than the e_g, antiferromagnetic interaction is possible where the magnetic b_{2g} orbital could overlap with the IM2py SOMO. According to the Angular Overlap Model (AOM) parameterization, the above orbital splitting is assumed when the π interaction energy ($2e_\pi$(imino) + $2e_\pi$(Cl)) for the b_{2g} orbital is larger than that (e_π(py) + e_π(Cl)) for the e_g; $2e_\pi$(imino) > e_π(py) − e_π(Cl), where the inequality is not necessarily unreasonable for cobalt(II) complexes even with the π donor character of pyridine.[35] In addition to the ferromagnetic interaction ($J_{d(z^2)\text{-}IM^F} + J_{d(x^2-y^2)\text{-}IM^F}$) resulting from orthogonality between the d(z^2) (e_g) and d($x^2 - y^2$) (e_g) orbitals and the IM2py SOMO, this antiferromagnetic contribution ($J_{d(b_{2g})\text{-}IM^{AF}}$) leads to reduction of the ferromagnetic interaction as compared with the reverse case ($J_{d(e_g)\text{-}IM^F}$) for the magnetic e_g orbital; *i.e.* $J = \frac{1}{3}(J_{d(z^2)\text{-}IM^F} + J_{d(x^2-y^2)\text{-}IM^F} + J_{d(b_{2g})\text{-}IM^{AF}}) < \frac{1}{3}(J_{d(z^2)\text{-}IM^F} + J_{d(x^2-y^2)\text{-}IM^F} + J_{d(e_g)\text{-}IM^F})$. This suggests some possibility to correlate the magnetic interactions with the ligand field or AOM parametrization.

UV-vis-NIR absorption spectra

The UV-vis-NIR absorption spectra of complexes **1**–**4** in CH_2Cl_2 at room temperature are shown together with that of free IM2py in Fig. 5. The similarity in spectral pattern between CH_2Cl_2 solution and the solid state indicates that the molecular structure of the complexes in the crystals, (*OC*-6-22)-*cis*(Cl)-*trans*(py)-[MCl_2(IM2py)$_2$], is retained also in CH_2Cl_2 solutions.

The d–d transition bands. Of two weak NIR bands of the nickel(II) complex **3** (Fig. 5), the lower energy band at 9670 cm^{-1} with $\varepsilon = 6.8$ dm^3 mol^{-1} cm^{-1} accompanied by a shorter wavelength broad shoulder is assigned as the first spin-allowed d–d ($^3A_2 \longrightarrow {}^3T_2$) transition band. The other rather sharper band observed at 12100 cm^{-1} with $\varepsilon = 9.2$ dm^3 mol^{-1} cm^{-1} presumably originates from an Ni(II)-centered spin-forbidden d–d ($^3A_2 \longrightarrow {}^1E$) transition. As compared with our recent study for Ni(II)–NIT2py complexes,[15] it is clear that the present IM2py complex **3** exhibits intensity enhancement for such a spin-forbidden d–d transition by borrowing MLCT intensities through magnetic exchange coupling with the radical unpaired electrons of the nitroxide. The exchange coupling between the

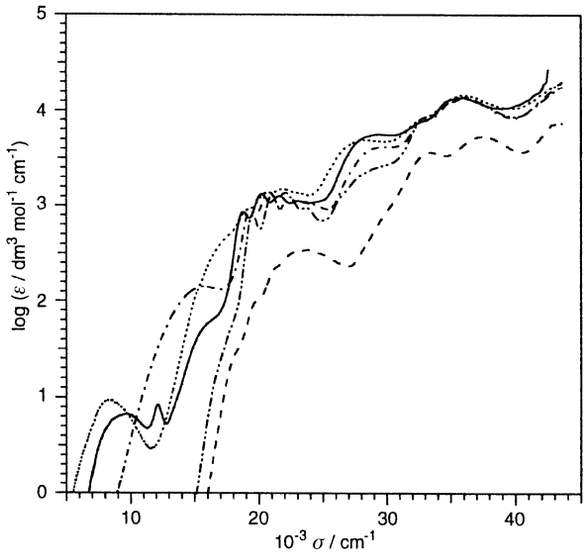

Fig. 5 UV-vis-NIR absorption spectra of complexes **1** (—·—·—), **2** (·····), **3** (———), **4** (–··–··–) and free IM2py (– – – –) in dichloromethane at 23 °C.

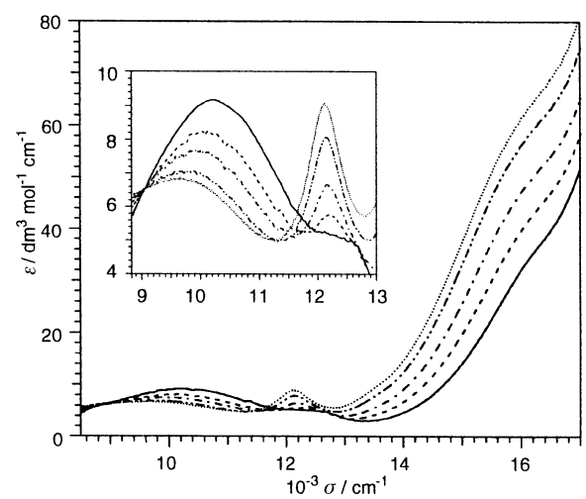

Fig. 6 Temperature dependence of the vis-NIR absorption spectrum of complex **3** in dichloromethane: 300 (·····), 275 (–··–··–), 250 (—·—·—), 225 (– – – –) and 200 K (———). The inset expands the d–d transition band region.

d electrons of Ni(II) and two of the IM2py unpaired electrons allows the Ni(II)-centered ground $^3A_2$ and excited ^1E states to split into four ($|\boldsymbol{S}, \boldsymbol{S}_R\rangle = |2, 1\rangle, |1, 1\rangle, |1, 0\rangle, |0, 1\rangle$) and two spin states ($|\boldsymbol{S}^*, \boldsymbol{S}_R\rangle = |1^*, 1\rangle, |0^*, 0\rangle$), respectively. Therefore, the originally spin-forbidden d–d $^3A_2 \longrightarrow {}^1E$ transition becomes spin-allowed due to the triplet–triplet $|1, 1\rangle$ or $|1, 0\rangle \longrightarrow |1^*, 1\rangle$ and singlet–singlet $|0, 1\rangle \longrightarrow |0^*, 0\rangle$ transitions with the same spin multiplicity.

For complex **3** with ferromagnetic interaction between Ni(II) and IM2py, the formally spin-forbidden band originating from the $^3A_2 \longrightarrow {}^1E$ transition is less intense ($\varepsilon = 9.2$ dm^3 mol^{-1} cm^{-1}) than that of the Ni(II)–NIT2py complexes with antiferromagnetic interaction ($\varepsilon > 100$ dm^3 mol^{-1} cm^{-1}), but larger than that found for the Cr(III)Ni(II)$_3$ tetranuclear compound with a smaller ferromagnetic interaction ($J = 5.3$ cm^{-1}).[36] Furthermore, the absorption band intensity of complex **3** decreased gradually on lowering the temperature (Fig. 6, inset) while that of the Ni(II)–NIT2py complexes increased, resulting from the different magnetic interactions between Ni(II) and the respective nitroxides. For complex **3** the electronic transitions from the lowest ground quintet state to the ^1E-based excited triplet and singlet states are actually forbidden. The depopulation of the triplet or singlet ground states decreases the band

intensity on cooling as expected. This is the first example to substantiate a ferromagnetically coupled system by the variable temperature absorption spectra. We are now attempting to make a quantitative analysis of the variable temperature intensity change in connection with the magnetic exchange parameter J.

The temperature dependence of the other NIR first spin-allowed d–d $^3A_2 \longrightarrow {}^3T_2$ absorption band of complex **3** gives some information about the magnetic interaction at the nickel(II) $^3T_2$ excited state, J^*. The band position was significantly blue-shifted by more than 450 cm^{-1} (from 9670 to 10130 cm^{-1}) and intensified by almost 1.5 times (from $\varepsilon = 6.6$ to 9.2 $dm^3\ mol^{-1}\ cm^{-1}$) on cooling from 300 to 200 K. This shift value is much larger than those of ordinary non-radical complexes; for instance, $[Ni(acac)_2(tmen)]$ (tmen = *N*,*N*,*N*′,*N*′-tetramethylethylenediamine) shows a blue-shift of only 180 cm^{-1} under the same condition. The larger blue-shift of complex **3** results probably from the weaker magnetic interaction at the $^3T_2$ excited state as compared to that at the $^3A_2$ ground state. This is not an unlikely assumption, since the magnetic interaction with two IM2py and each unpaired d electron in the dσ (e_g) and dπ (t_{2g}) orbitals for the $^3T_2$ excited state would lead to some reduction of the ferromagnetic interaction and conversely to the appearance of the antiferromagnetic one, respectively, the summation resulting in the decrease in J^* value. In such a situation the spin-allowed quintet–quintet transition requires higher energy than the triplet–triplet or singlet–singlet transition, and the intensity of the quintet–quintet transition becomes larger at lower temperature in view of the ground quintet state.

For the cobalt(II) complex **2** the NIR absorption band at 8460 cm^{-1} ($\varepsilon = 9.3\ dm^3\ mol^{-1}\ cm^{-1}$) following a higher energy broad shoulder is due to the first spin-allowed d–d $^4T_1 \longrightarrow {}^4T_2$ transition (Fig. 5). This band maximum and shoulder seem to correspond to the holohedrized tetragonal splitting components for the high-spin cobalt(II) complex. Similarly to the nickel(II) complex **3**, the absorption band showed a remarkable blue-shift, from 8460 cm^{-1} at 300 K to 9180 cm^{-1} at 200 K (Fig. S2 in ESI). This is also correlated with the newly appeared spin states due to magnetic interactions between the Co(II) and two IM2-py radicals.

The charge-transfer transition bands. In addition to the d–d absorption bands described above, the complexes of Mn(II), Co(II) and Ni(II) **1**–**3** showed another band or shoulder in the 14000–17000 cm^{-1} region. Complex **3** gave a shoulder around 16000 cm^{-1} (Figs. 5 and 6). The intensity of this shoulder became weaker on cooling. This fact indicates that the excited state of this transition does not include a quintet state, leading to the spin-allowed transition from the depopulated next-lowest ground triplet state to the excited triplet CT state or nickel(II) dσ to IM2py SOMO π*(N–O) CT (Scheme 2), the transition

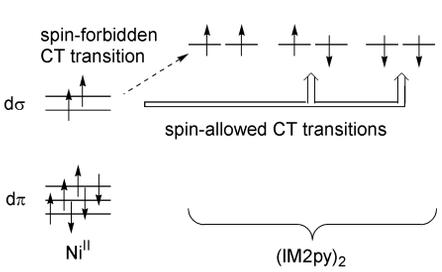

Scheme 2 The spin-allowed and spin-forbidden CT transitions for $[NiCl_2(IM2py)_2]$.

from the lowest quintet state being spin-forbidden. This result substantiates the ferromagnetic interaction as inferred from the magnetic susceptibility measurement.

The cobalt(II) complex **2** exhibits variable temperature behaviour for the shoulder around 15000 cm^{-1} similar to that for the 16000 cm^{-1} shoulder of the nickel(II) complex **3**; the intensity decreased on lowering the temperature (Fig. S2 of ESI), resulting in a spin-allowed transition from the depopulated next-lowest ground quartet state to the excited quartet CT state with antiferromagnetic configuration (*vide supra*), the transition from the lowest sextet state being spin-forbidden. This may be due to the cobalt(II) dσ to IM2py SOMO π*(N–O) CT transition, as for the nickel(II) complex. From this spectroscopic behaviour a ferromagnetic interaction between Co(II) and IM2py radicals is verified in accordance with the magnetic susceptibility measurement.

The corresponding absorption spectrum of manganese(II) complex **1** was observed as a broad band at 15710 cm^{-1}. In contrast to the behaviour of the complexes of Ni(II) and Co(II), the band intensity became larger on cooling (Fig. S3 of ESI), leading to a spin-allowed transition from the lowest ground quartet state to the excited quartet state. This is consistent with the antiferromagnetic interaction between Mn(II) and IM2py as demonstrated by the magnetic susceptibility measurement. It is not clear whether the absorption band is due to the CT transition from the manganese(II) dσ or dπ to SOMO π*(N–O).

Concluding remarks

For the newly prepared bis(IM2py) complexes, stereospecific formation with *cis*(Cl)-*trans*(py) geometrical structure is demonstrated. The magnetic interactions between two IM2py in zinc(II) complex **4** and between Mn(II), Co(II) or Ni(II) and IM2py in complexes **1**, **2** and **3** are elucidated by the variable temperature magnetic susceptibilities in combination with the temperature-dependent UV-vis-NIR spin-forbidden or spin-allowed d–d transitions and the dσ or dπ to IM2py SOMO CT.

Acknowledgements

We gratefully acknowledge support of this research by a Grant-in-Aid for Scientific Research (No.10304056) from the Ministry of Education, Science and Culture.

References

1 A. Caneschi, D. Gatteschi and P. Rey, *Prog. Inorg. Chem.*, 1991, **39**, 331.
2 D. Luneau, G. Risoan, P. Rey, A. Grand, A. Caneschi, D. Gatteschi and J. Laugier, *Inorg. Chem.*, 1993, **32**, 5616.
3 C.-F. Huang and H.-H. Wei, *J. Chin. Chem. Soc. (Taipei)*, 1997, **44**, 439.
4 S. Ohba, T. Kato, N. Yoshioka and H. Inoue, *Acta Crystallogr., Sect. C*, 1997, **53**, CIF-access paper, IUC9700004.
5 P. F. Richardson and R. W. Kreilick, *J. Am. Chem. Soc.*, 1977, **99**, 8183.
6 F. L. de Panthou, E. Belorizky, R. Calemczuk, D. Luneau, C. Marcenat, E. Ressouche, P. Turek and P. Rey, *J. Am. Chem. Soc.*, 1995, **117**, 11247.
7 B.-W. Sun, Q.-H. Zhao, D.-Z. Liao, Z.-H. Jiang, S.-P. Yan, G.-L. Wang, X.-K. Yao and H.-G. Wang, *Can. J. Chem.*, 2000, **78**, 322.
8 A. Caneschi, D. Gatteschi and R. Sessoli, *Inorg. Chem.*, 1993, **32**, 4612; N. C. Schiødt, F. F. de Biani, A. Caneschi and D. Gatteschi, *Inorg. Chim. Acta*, 1996, **248**, 139.
9 K. Fegy, D. Luneau, T. Ohm, C. Paulsen and P. Rey, *Angew. Chem., Int. Ed.*, 1998, **37**, 1270; K. Fegy, N. Sanz, D. Luneau, E. Belorizky and P. Rey, *Inorg. Chem.*, 1998, **37**, 4518; K. Fegy, D. Luneau, E. Belorizky, M. Novac, J.-L. Tolence, C. Paulsen, T. Ohm and P. Rey, *Inorg. Chem.*, 1998, **37**, 4524.
10 C. Rancurel, D. B. Leznoff, J.-P. Sutter, S. Golhen, L. Ouahab, J. Kliava and O. Kahn, *Inorg. Chem.*, 1999, **38**, 4753; C. Rancurel, D. B. Leznoff, J.-P. Sutter, P. Guionneau, D. Chasseau, J. Kliava and O. Kahn, *Inorg. Chem.*, 2000, **39**, 1602.
11 A. Caneschi, P. Chiesi, L. David, F. Ferraro, D. Gatteschi and R. Sessoli, *Inorg. Chem.*, 1993, **32**, 1445.
12 D. Luneau, F. M. Romero and R. Ziessel, *Inorg. Chem.*, 1998, **37**, 5078.

13 G. Francese, F. M. Romero, A. Neels, H. Stoeckli-Evans and S. Decurtins, *Inorg. Chem.*, 2000, **39**, 2087.
14 M. Tanaka, K. Matsuda, T. Itoh and H. Iwamura, *Angew. Chem., Int. Ed.*, 1998, **37**, 810.
15 T. Yoshida, K. Kanamori, S. Takamizawa, W. Mori and S. Kaizaki, *Chem. Lett.*, 1997, 603; T. Yoshida, T. Suzuki, K. Kanamori and S. Kaizaki, *Inorg. Chem.*, 1999, **38**, 1059; T. Yoshida, T. Suzuki, K. Kanamori and S. Kaizaki, *Inorg. Chem.*, 1999, **38**, 5926.
16 T. Yoshida and S. Kaizaki, *Inorg. Chem.*, 1999, **38**, 1054.
17 C. Lescop, D. Luneau, G. Bussière, M. Triest and C. Reber, *Inorg. Chem.*, 2000, **39**, 3740.
18 C. Mathonière, O. Kahn, J.-C. Daran, H. Hilbig and F. H. Köhler, *Inorg. Chem.*, 1993, **32**, 4057; C. Mathonière and O. Kahn, *Inorg. Chem.*, 1994, **33**, 2103; O. Cador, C. Mathonière and O. Kahn, *Inorg. Chem.*, 1997, **36**, 1923; O. Cador, C. Mathonière, O. Kahn, J.-P. Costes, M. Verelst and P. Lecante, *Inorg. Chem.*, 1999, **38**, 2643.
19 O. Cador, C. Mathonière and O. Kahn, *Inorg. Chem.*, 2000, **39**, 3799.
20 D. Luneau, P. Rey, J. Laugier, P. Fries, A. Caneschi, D. Gatteschi and R. Sessoli, *J. Am. Chem. Soc.*, 1991, **113**, 1245.
21 D. Luneau, P. Rey, J. Laugier, E. Belorizky and A. Conge, *Inorg. Chem.*, 1992, **31**, 3578.
22 A. Caneschi, D. Gatteschi, J. Laugier, P. Rey and C. Zanchini, *Inorg. Chem.*, 1989, **28**, 1969.
23 D. Luneau, F. M. Romero and R. Ziessel, *Inorg. Chem.*, 1998, **37**, 5078.
24 A. Marvilliers, Y. Pei, J. C. Boquera, K. E. Vostrikova, C. Paulsen, E. Rivière, J.-P. Audière and T. Mallah, *Chem. Commun.*, 1999, 1951.
25 K. E. Vostrikova, D. Luneau, W. Wernsdorfer, P. Rey and M. Verdaguer, *J. Am. Chem. Soc.*, 2000, **122**, 718.
26 H. Oshio, A. Ohto and T. Ito, *Chem. Commun.*, 1996, 1541.
27 H. Oshio, T. Watanabe, A. Ohto, T. Ito and U. Nagashima, *Angew. Chem., Int. Ed. Engl.*, 1994, **33**, 670; H. Oshio, T. Watanabe, A. Ohto, T. Ito, T. Ikoma and S. Tero-Kubota, *Inorg. Chem.*, 1997, **36**, 3014.
28 E. F. Ullman, J. H. Osiecki, D. G. B. Boocock and R. Darcy, *J. Am. Chem. Soc.*, 1974, **94**, 7049; E. F. Ullman, L. Call and J. H. Osiecki, *J. Org. Chem.*, 1970, **35**, 3623.
29 G. M. Sheldrick, *Acta Crystallogr., Sect. A*, 1990, **46**, 467.
30 G. M. Sheldrick, SHELXL 97, University of Göttingen, 1997.
31 Y. Yamamoto, T. Yoshida, T. Suzuki and S. Kaizaki, unpublished work.
32 R. D. Shannon, *Acta Crystallogr., Sect. A*, 1976, **32**, 751.
33 Y. Yamamoto, T. Suzuki and S. Kaizaki, unpublished work.
34 O. Kahn, *Molecular Magnetism*, VCH, New York, 1993.
35 A. Bencini, C. Benelli and D. Gatteschi, *Coord. Chem. Rev.*, 1984, **60**, 131.
36 Y. Pei, Y. Journaux and O. Kahn, *Inorg. Chem.*, 1989, **28**, 100.